ISBN: 978-3-95450-216-5 doi:10.18429/JACoW-eeFACT2018-MOYBA01

ROUND COLLIDING BEAMS AT VEPP-2000 WITH EXTREME TUNESHIFTS

D. Shwartz†[1], V. Anashin, O. Belikov, D. Berkaev, K. Gorchakov, A. Kasaev, A. Kirpotin, I. Koop[1], A. Krasnov, G. Kurkin, A. Lysenko, S. Motygin, E. Perevedentsev[1], V. Prosvetov, D. Rabusov, Yu. Rogovsky[1], A. Semenov, A. Senchenko[1], D. Shatilov, P. Shatunov, Yu. Shatunov[1], O. Shubina, M. Timoshenko, I. Zemlyansky, Yu. Zharinov

Budker Institute of Nuclear Physics, Novosibirsk, 630090, Russia
[1]also at Novosibirsk State University, Novosibirsk, 630090, Russia

Abstract

VEPP-2000 is the only electron-positron collider operating with round beams that results in enhancement of beam-beam limit. VEPP-2000 with SND and CMD-3 detectors carried out two successful data-taking runs after new BINP injection complex was commissioned. The 2016/2017 run was dedicated to high energy range (640-1000 MeV per beam) while the 2017/2018 run was focused at 275-600 MeV/beam energies. With sufficient positron production rate and upgraded full-energy booster the collider luminosity was limited by beam-beam effects, namely flip-flop effect. Thorough machine tuning together with new ideas introduced to suppress flip-flop allowed to achieve high beam-beam tuneshift and bunch-by-bunch luminosity values at specific beam energies. The achieved luminosity increased 2-5 times in a whole energy range in comparison to phase-1 operation (2010-2013).

ROUND COLLIDING BEAMS

The VEPP-2000 collider [1-3] exploits the round beam concept (RBC) [4] firstly proposed for the Novosibirsk Phi-factory project [5]. This approach, in addition to the straightforward geometrical gain factor in luminosity should yield the beam-beam limit enhancement. An axial symmetry of the disruptive nonlinear counter-beam force together with the X–Y symmetry of the transfer matrix between the two IPs provide an additional integral of motion, namely, the longitudinal component of angular momentum $M_z = x'y - xy'$. Although the particles' dynamics remain strongly nonlinear due to beam-beam interaction, it becomes effectively one-dimensional. The reduction of degrees of freedom thins out the resonance grid and suppress the diffusion rate resulting finally in a beam-beam limit enhancement [6].

Thus, there are several demands upon the storage ring lattice suitable for the RBC:

1. Head-on collisions (zero crossing angle).
2. Small and equal β functions at IP ($\beta^*_x = \beta^*_y$).
3. Equal beam emittances ($\varepsilon_x = \varepsilon_y$).
4. Equal fractional parts of betatron tunes ($\nu_x = \nu_x$).

The first three requirements provide the axial symmetry of collisions while requirements (2) and (4) are needed for X–Y symmetry preservation between the IPs.

VEPP-2000 OVERVIEW

VEPP-2000 is a small 24 m perimeter single-ring collider operating in one-by-one bunch regime in the energy range below 1 GeV per beam. Its layout is presented in Fig. 1-2. Collider itself hosts two particle detectors [7, 8], Spherical Neutral Detector (SND) and Cryogenic Magnetic Detector (CMD-3), placed into dispersion-free low-beta straights. The final focusing (FF) is realized using superconducting 13 T solenoids. The main design collider parameters are listed in Table 1.

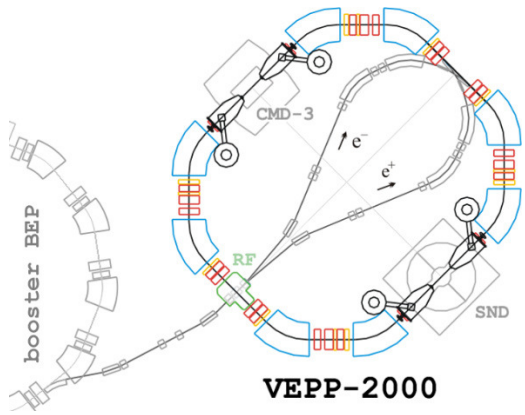

Figure 1: VEPP-2000 storage ring layout.

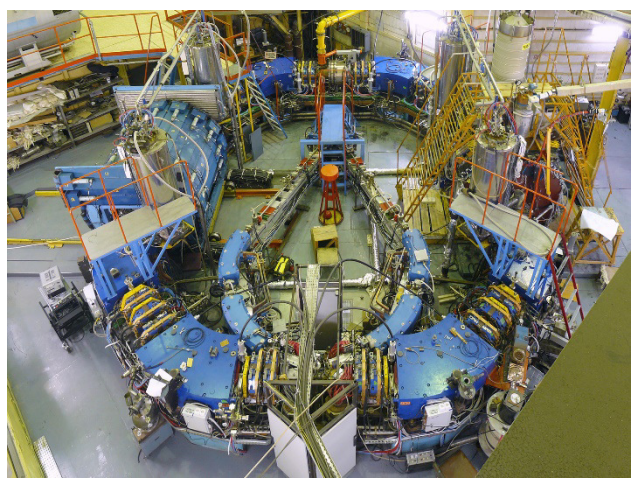

Figure 2: VEPP-2000 collider photo.

† d.b.shwartz@inp.nsk.su

ISBN: 978-3-95450-216-5 doi:10.18429/JACoW-eeFACT2018-MOYBA01

Table 1: VEPP-2000 Design Parameters (at E = 1 GeV)

Parameter	Value
Circumference, C	24.39 m
Energy range, E	150–1000 MeV
Number of bunches	1 × 1
Number of particles per bunch, N	1×10^{11}
Betatron functions at IP, $\beta^*_{x,y}$	8.5 cm
Betatron tunes, $\nu_{x,y}$	4.1, 2.1
Beam emittance, $\varepsilon_{x,y}$	1.4×10^{-7} m rad
Beam–beam parameters, $\xi_{x,z}$	0.1
Luminosity, L	1×10^{32} cm^{-2} s^{-1}

Injection Chain Upgrade

During commissioning and first operation phase in 2010-2013 VEPP-2000 used old positron production and injection chain that restricted available positron beam intensity and limited the luminosity at energy range above 500 MeV. Since 2016 VEPP-2000 is linked to the new BINP injection complex (IC) [9, 10] via long transfer channel. In addition, the booster BEP was upgraded in order to increase top energy up to 1 GeV and perform top-up injection [11].

Circular Modes

The RBC at VEPP-2000 was implemented by placing two pairs of superconducting focusing solenoids into two interaction regions (IR) symmetrically with respect to collision points. There are several combinations of solenoid polarities that satisfy the round beams' requirements: "normal round" (++ −−), "Möbius" (++ −+) and "double Möbius" (++ ++) options rotate the betatron oscillation plane by ±90° and give alternating horizontal orientation of the normal betatron modes outside the solenoid insertions.

Two "flat" combinations (+− +− or +− −+) also satisfy the RBC approach if the betatron tunes lie on the coupling resonance $\nu_x - \nu_y = 2$ to provide equal emittances via residual X-Y coupling.

Unfortunately, options with mode rotations suffer from serious limitation of the dynamic aperture (DA). Thus hereafter we will suppose conventional "flat" mode (+− −+) with equal emittance due to tunes chosen at the main coupling resonance.

Short Solenoids

Each of four solenoid knobs in fact consists of several coils [12]. The small very forward coil is used to compensate the longitudinal field of CMD-3 detector. The main coil is split in longitudinal direction into two parts powered in series with middle point brought out to room-temperature commutation deck for quench control. At the beam energy range below 600 MeV it is possible to use only forward parts of main coils that helps effectively to move final focusing closer to IP.

All the solenoids configuration changes ("flat" to "möbius", "long" to "short") unfortunately results in strong closed orbit distortion and needs solenoids beam-based realignment.

Machine Tuning

VEPP-2000 operates in a wide energy range with strong saturation of magnetic elements at the top energy. In contrast, at low energies the fixed 1.3 T longitudinal field of CMD-3 detector significantly disturbs the focusing. Thus while energy scanning to achieve high machine performance of great importance is the machine tuning at each energy level. The lattice functions correction including X-Y coupling is made at VEPP-2000 using Orbit Response Matrix (ORM) analysis [13].

The ORM is used also to determine and correct closed orbit at quadrupoles by varying their strength, thus using them as additional BPMs. The similar technique is used for final beam-based alignment of solenoids.

Very important it turned out to minimize the dipole correctors' currents, done with help of ORM as well. The reason is poor quality of the steering coils being embedded in quadrupoles due to lack of space.

FLIP-FLOP EFFECT

The final beam-beam limit at VEPP-2000 corresponds to the onset of a flip-flop effect [14]: the self-consistent situation when one of the beam size is blown-up while another beam size remains almost unperturbed. The simple linear model of flip-flop was discussed earlier [15], with a very high threshold intensity. Observed in VEPP-2000 behavior is most likely caused by an interplay of beam-beam interaction and nonlinear lattice resonances.

In Fig. 3 images from the online control TV camera are presented for the cases of regular beams (a), blown-up electron beam (b) or positron beam (c). The corresponding coherent oscillations spectra are shown on the right. One can see in the spectra of a slightly kicked bunch that the shifted tune (π-mode) sticks to the 1/5 resonance in the case of a flip-flop.

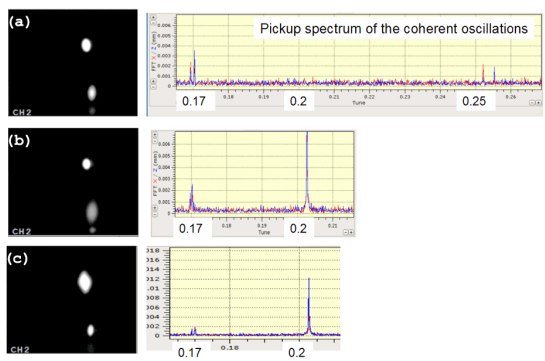

Figure 3: Coherent beam-beam oscillations spectra.

The flip-flop threshold is sensitive to several tuning knobs, in particularly to X-Y coupling and beta-functions misbalance at IP. In addition, the influence of bunch length on the threshold was observed.

ISBN: 978-3-95450-216-5 doi:10.18429/JACoW-eeFACT2018-MOYBA01

BUNCH LENGTHENING

While studying the dependence of beam-beam effects on bunch length at relatively low energy of 392.5 MeV it was found that the RF voltage decrease from 30 kV to 17 kV gives a significant benefit in beams intensity and luminosity threshold.

This enhancement with lower voltage comes from the bunch lengthening. In our particular case, this lengthening is the result of several effects. In addition to regular growth of radiative bunch length with voltage two collective effects take place: potential well distortion and microwave instability. The latter one is observed at low energies with a low RF voltage above a certain bunch intensity [16, 17]. In Fig. 4 the measured by dissector bunch length dependence on beam current is presented for two levels of RF voltage. In Fig. 5 the extracted from transverse horizontal beam size measurements energy spread as a function of intensity is shown. Red points correspond to microwave instability above the threshold.

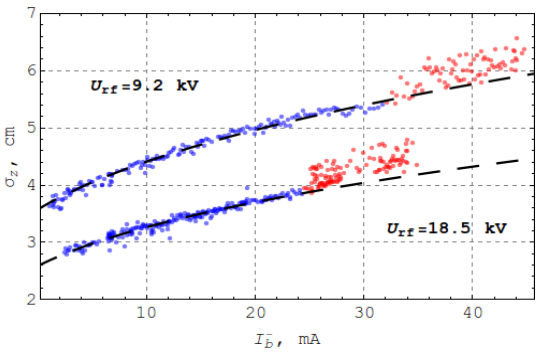

Figure 4: Bunch length as a function of beam current @ E = 480 MeV.

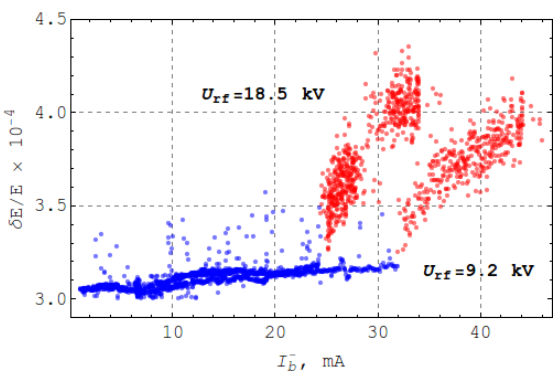

Figure 5: Beam energy spread as a function of beam current @ E = 480 MeV.

The analysis of logged data was done at the energy of 392.5 MeV where enough data was stored for short (a) and long (b) bunch cases. Only "strong-strong" data was selected, i.e. the beam currents difference does not exceed 10%. In Fig. 6 the measured vertical sizes of electron (σ_{4M1Ly}) and positron (σ_{1M1Ry}) beams as a function of beam currents geometric average are shown.

One can see that in both cases the flip-flop develops (unequal positron and electron beam sizes) for beams intensity higher than 15 mA that corresponds to $\xi_{nom} \sim 0.1$. But the longer bunch tends to mitigate this effect for higher intensities.

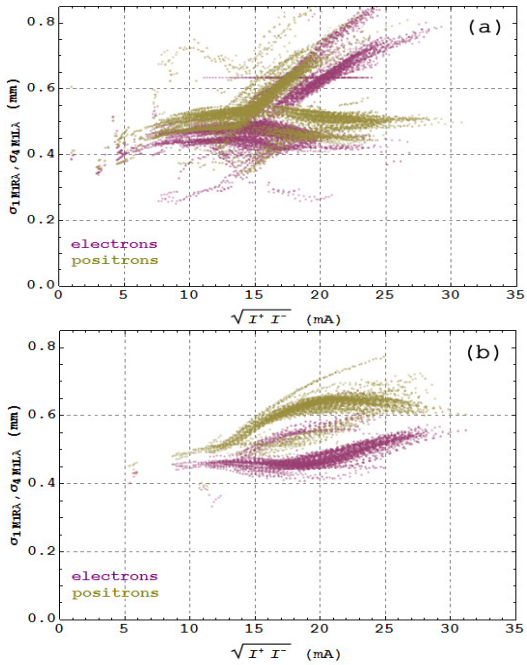

Figure 6: Beam sizes vs. beam current.

BEAM SHAKING

While taking data at low energy range where the radiative emittance is small but significant beta-squeeze is not allowed due to the DA shrinking thus leaving mechanical aperture not fully used the natural desire appeared to increase the emittance. It allows to increase the beam current with fixed particles density, i.e. with fixed at the threshold beam-beam parameter, and to increase luminosity linearly to beam intensity.

Due to very tight components arrangement there is no room to install the wiggler for emittance excitation as it was done at VEPP-2M [18]. The idea was proposed to kick the beam weakly (in comparison to beam size) and frequently (in comparison to damping time). In the presence of strong nonlinear forces of colliding beam after the single kick the excited coherent oscillation decoheres very quickly thus increasing effective beam emittance. This method was probably firstly proposed and tested in 1960-s at VEP-1 collider [19].

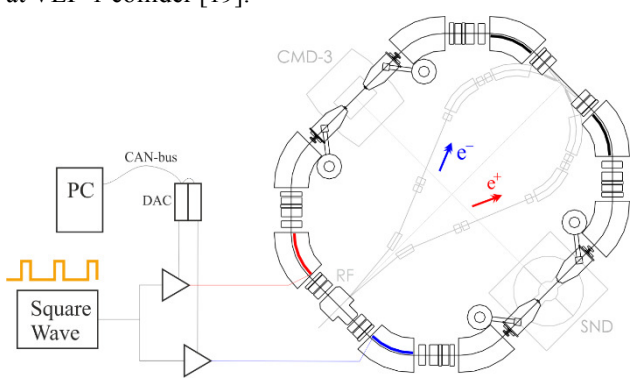

Figure 7: The scheme of beam shaking.

ISBN: 978-3-95450-216-5 doi:10.18429/JACoW-eeFACT2018-MOYBA01

During complex upgrade in order to obtain injection at top energy two additional kicker plates were installed inside dipoles opposite to injection region (see Fig. 7). At low energy the plates are not in use. The square wave generator was used to produce pulses of ~300 ns duration. Separated and amplified independently in two channels by software controlled amplificators pulses are applied to the plates in a running wave manner to affect only on one beam per channel. In fact, in routine operation inevitably both beams are affected via beam-beam interaction.

The typical pulses parameters are the following: pulse duration ~300 ns (3-4 turns), repetition rate $(50\ \mu s)^{-1}$, pulse amplitude 50-100 V (depends on beam energy).

The example of beam behavior observed by pickup at 360 MeV with shaker switched on is presented in Fig. 8. Here the opposite beam is absent, kicks excite horizontal oscillations (red). One can see the fast swap to vertical oscillations (blue) due to operating at coupling resonance and relatively fast decoherence due to machine nonlinearities.

The spectrum becomes line spectrum due to presence of several kicks periodically exciting oscillations during the period of Fourier analysis.

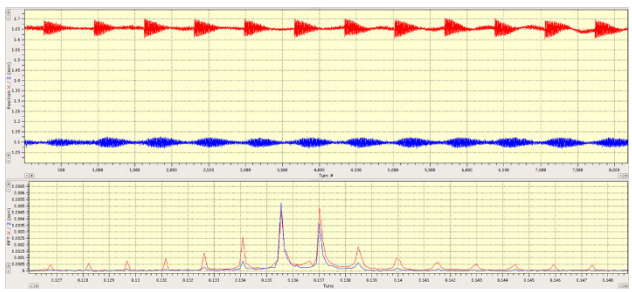

Figure 8: The signal of the single beam shaking at pickup and its Fourier spectrum.

Next Fig. 9 shows the pickup signal fragment of 274 MeV beam being shaken in the collision regime. The single kick excites oscillation with ~30 μm amplitude which decoheres during ~50 turns. At this energy the beam size is equal to 250 μm while the damping time 130 ms corresponds to 1.6×10^6 turns.

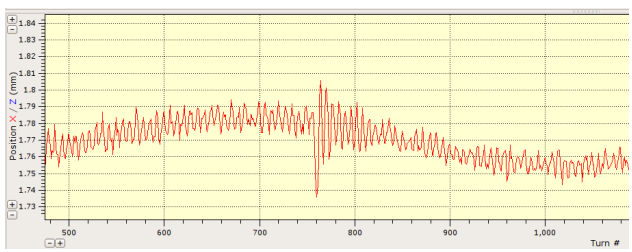

Figure 9: The signal of the single beam shaking at pickup and its Fourier spectrum. The slow oscillation corresponds to synchrotron motion.

The beam shaking experimentally results in beams emittance growth. This growth depends on the controllable shaker parameters (pulse amplitude, pulse duration, repetition rate). The properly increased emittance prevents the flip-flop development during injection cycle: the "strong" beam can't shrink to unperturbed size when "weak" beam oscillates with large amplitudes. In addition the beam lifetime is improved due to Touschek scattering is suppressed with increased emittance.

LUMINOSITY AND BEAM-BEAM PARAMETER

As a result of beam shaking technique implementation the beams intensities and luminosity at low energy range increased significantly. In Fig. 10 the luminosity is presented achieved in 2013 and in 2018 at the same given energy of 391-391 MeV.

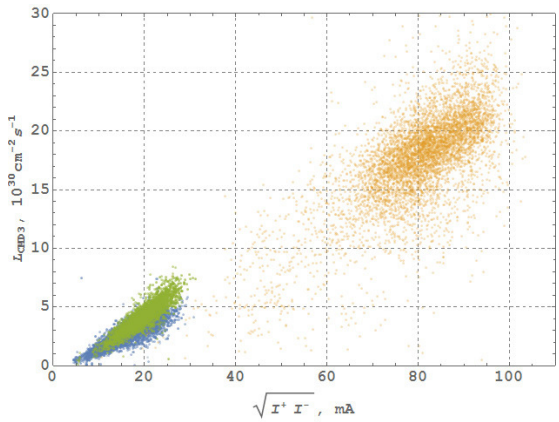

Figure 10: The CMD-3 recorded luminosity as a function of beam currents. Blue and green dots correspond to machine performance in 2013 with short and long bunch correspondingly. Yellow dots corresponds to 2018.

The luminosity increased linearly with the current growth in spite of the naïve expectation of quadratic dependence from the expression for round beam:

$$L = \frac{N^+ N^-}{4\pi\sigma^{*2}} f_0 , \qquad (1)$$

that is an evidence of beam size growth driven by beam-beam interaction.

For the measured luminosity and beams intensities we can extract from (1) the real beam size which indeed shows the linear growth with intensity (see Fig. 11).

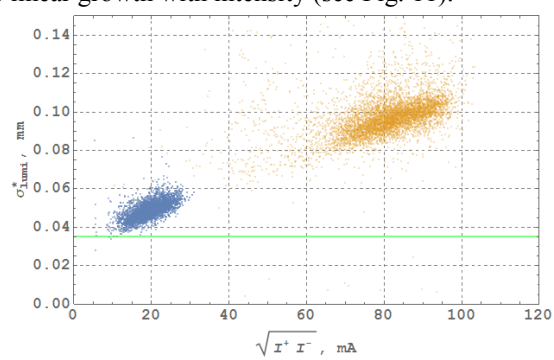

Figure 11: Beam size at IP extracted from CMD-3 luminosity. Blue and yellow dots corresponds to 2013 and 2018 data. Green line show the design beam size value.

ISBN: 978-3-95450-216-5 doi:10.18429/JACoW-eeFACT2018-MOYBA01

With beam size extracted from luminosity measurements we can define the "achieved" beam-beam parameter as:

$$\xi_{\text{lumi}} = \frac{N^- r_e \beta^*_{\text{nom}}}{4\pi\gamma\sigma^{*2}_{\text{lumi}}}, \quad (2)$$

where the beta function is nominal design value at IP. In addition we can define "nominal ξ" in a similar way:

$$\xi_{nom} = \frac{N^- r_e \beta^*_{\text{nom}}}{4\pi\gamma\sigma^{*2}_{nom}}, \quad (3)$$

where beam size is unperturbed. Due to strong emittance and beam size growth ξ_{nom} has nothing to do with real beam-beam tuneshifts being just a beam intensity normalized to clean out the dependence on energy.

We can now express directly the luminosity via beam-beam parameter:

$$L = \frac{N f_0 \gamma}{r_e} \frac{\xi_{lumi}}{\beta^*_{nom}}. \quad (4)$$

Finally, the achieved beam-beam parameter extracted from luminosity at 391-392 MeV is presented in Fig. 12. It saturates strongly and doesn't exceed 0.08.

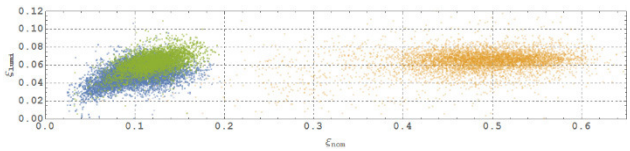

Figure 12: Beam-beam parameter extracted from CMD-3 luminosity. Notation is the same as in Fig. 11.

COHERENT MODES

The cross-check for the acting beam-beam parameter value can be done through the analysis of the coherent beam oscillation spectrum. Usually we excite eigen modes with tiny kick, but with constant beam shaking modes tunes are always visible in pickup signal spectra. In Fig. 13 the example of coherent spectrum and spectrogram at beam energy of 360 MeV are shown. Left peak corresponds to so called σ-mode with unperturbed betatron tune 0.135 while the right peak indicate the π-mode with shifted tune to 0.345. The total tuneshift is $\Delta\nu = 0.21$.

Figure 13: Beam-beam modes spectrum @ 360 MeV.

With given incoherent beam-beam parameter ξ_{inc}, i.e. parameter that is seen by the single particle interacting with opposite "strong" beam, the coherent beam-beam parameter will be

$$\xi_{coh} = 2 \cdot \frac{1}{2} \cdot Y \cdot \xi_{inc}, \quad (5)$$

where factor 2 shows that the distance between two beams centroids is twice larger than coordinate shift in π-eigen mode; factor ½ ("Hirata's one half") appears due to the proper averaging over Gaussian distribution in the model of two rigid Gaussian beams [20]; Yokoya factor Y is responsible for transverse distribution deformation during the oscillation excitation [21].

We assume that Y = 1 since the oscillations with very small amplitude (~5 μm = 0.1 σ^*) were excited by a fast kick and the spectrum was investigated for only 8000 turns that is much shorter than damping time. During this short time beam distribution is not deformed by an oscillating counter beam. This assumption was studied thoroughly at VEPP-2M [22]. First simulations by *Lifetrac* code [23] in quasi-strong-strong regime also do not show significant deviation of Y-factor from unity.

Finally, with the given modes' tunes calculated ξ per one IP is equal to:

$$\xi = \frac{\cos(\pi\nu_\sigma) - \cos(\pi\nu_\pi)}{2\pi \sin(\pi\nu_\sigma)} \quad 0.17, \quad (6)$$

that is twice higher than beam-beam parameter defined from luminosity measurements. This discrepancy in not yet understood. However, the coherent tuneshift is routinely used for the machine fine tuning including beamshaker amplitude and completely correlates with luminosity maximization.

DATA COLLECTION

The 2016/17 run was the first data taking VEPP-2000 run with new injector [24-27]. It was dedicated to energy range from 640 MeV to 1003.5 MeV per beam. The design top energy was exceeded in order to achieve the mass of D^{*0}(2007). The run 2017/18 was dedicated to the data collection at low beam energies: 274 – 600 MeV. Fig. 14 presents the online status web-page during regular operation at 395.5 MeV energy in May 2018.

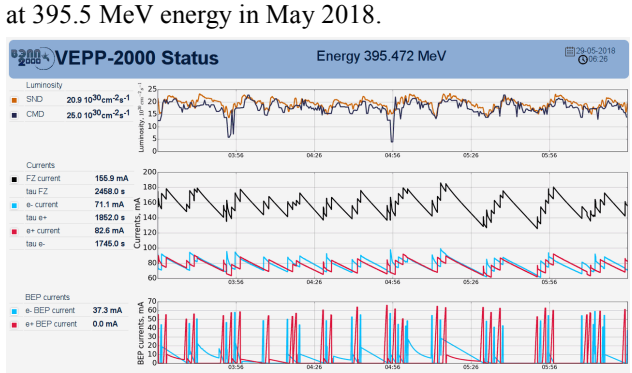

Figure 14: VEPP-2000 operation @ 395 MeV.

ISBN: 978-3-95450-216-5 doi:10.18429/JACoW-eeFACT2018-MOYBA01

The achieved luminosity in comparison to 2010-2013 performance is shown in Fig. 15. In the middle energy range the achieved luminosity is well above all expectations. At the same time at top energy luminosity is lower than design value in a factor of two.

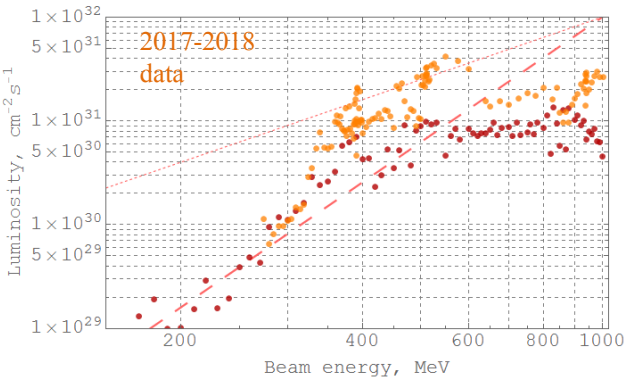

Figure 15: CMD-3 recorded in 2010-2013 (crimson) and in 2017-2018 (orange) luminosity averaged over 10% of best runs. Pink lines show scaling laws with fixed and variable β*.

The next figure presents the integrated luminosity as compared for several operating years. One should beware of direct comparison of integrals due to luminosity dependence on energy. 2012/13 and 2017/18 runs were spent for data taking below 500 MeV while the others were dedicated to higher energies.

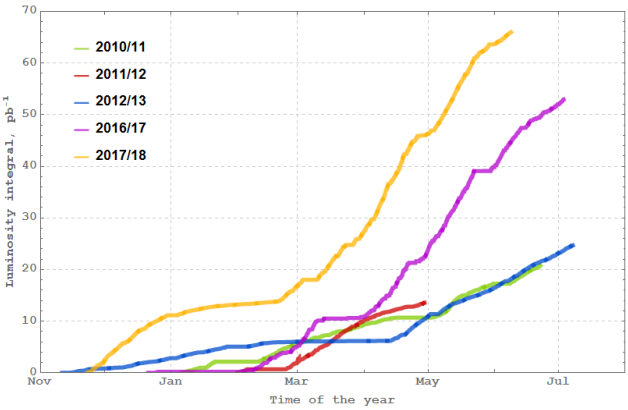

Figure 16: CMD-3 recorded luminosity integral.

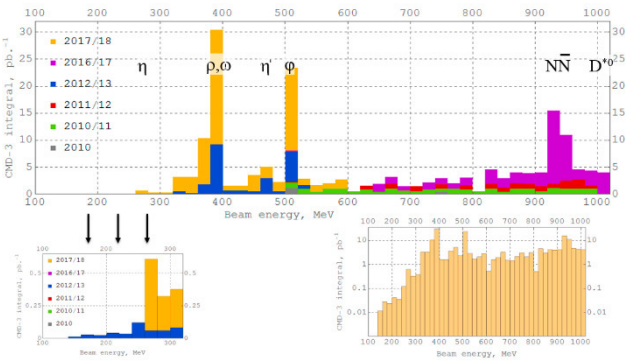

Figure 17: CMD-3 recorded luminosity integral.

The distribution of luminosity integral over energy is presented in Fig. 17. Although all the energy range is already covered mainly integral sticks to several points of interest such as different light mesons masses and threshold of nucleon-antinucleon production [28-30].

STREAK CAMERA

Recently the streak camera was installed at VEPP-2000 at one of the SR output (e⁻ direction) in parallel to regular CCD-camera [31]. The first studies were carried out at the energy of 392.5 MeV, with beamshaker switched off. While observing the single electron circulating beam with intensity above beam-beam threshold the positron bunch with the same intensity was injected. The latter's lifetime is very short, several milliseconds, due to beam-beam interaction. The single-turn snapshots of electron beam vertical-to-longitudinal distribution were made by streak camera at the chosen turn number after injection. In Fig. 18 the bunch profile is presented at 40th and 80th turn. Unfortunately significantly longer delays were not available with current hardware.

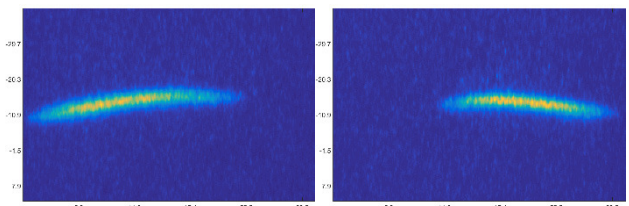

Figure 18: Streak camera e⁻ bunch profiles. Vertical/horizontal axis corresponds to vertical/longitudinal coordinate, both in arbitrary units.

It is clearly seen that bunch acquires a vertical tilt and this tilt oscillates very fast if compared to synchrotron motion. The synchrotron tune during this study was $\nu_s = 0.002$ thus equivalent to 500 turns. The tilt should exist not exclusively in vertical plane since the colliding beams are round, i.e. X-Y-symmetric, but streak camera was not able to observe horizontal coordinate.

For inverse situation when electron bunch is injected to the storage ring with circulating positron bunch the disruption is even worse. Distribution can be split into two parts as presented in Fig. 19.

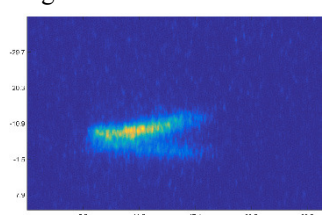

Figure 19: Injected e⁻ bunch in the presence of circulating intensive e⁺ bunch.

These first observations in addition to mentioned above influence of bunch length on beam-beam threshold indicates the importance of longitudinal motion on beam-beam effects. We plan to continue studies with streak-camera.

ISBN: 978-3-95450-216-5 doi:10.18429/JACoW-eeFACT2018-MOYBA01

CONCLUSION

Round beams give a serious luminosity benefit. VEPP-2000 with new BINP injector and upgraded booster started data taking in all energy range of 200–1000 MeV with a luminosity increased in a factor of 2-5. Novel technique ("beamshaking") for effective emittance control allow to suppress flip-flop effect and increase beams intensity at middle energies. Strong discrepancy between coherent and incoherent beam-beam parameter ξ is observed: problem to be solved. First studies with streak-camera have shown fast oscillating longitudinal bunch tilts. Upcoming new run will be devoted to energy range above 500 MeV with intent to achieve the target luminosity at top energy.

ACKNOWLEDGEMENT

We are grateful to A.M. Batrakov, D.B. Burenkov, I.N. Churkin, P.V. Logachev, M.I. Nepomnyaschikh, A.L. Romanov, V.S. Seleznev, A.N. Skrinsky, Yu.M. Velikanov, V.D. Yudin for continuous support.

This work is partially supported by Russian Science Foundation under project N 14-50-00080.

REFERENCES

[1] Yu.M. Shatunov *et al*., "Project of a New Electron-Positron Collider VEPP-2000", in *Proc. EPAC'00*, Vienna, Austria, 2000, pp. 439-441.

[2] D. E. Berkaev *et al.,*"The VEPP-2000 electron-positron collider: First experiments", *J. Exp. Theor. Phys.*, Vol.113, no.2, p.213 (2011)

[3] D. Shwartz *et al*., "Implementation of Round Colliding Beams Concept at VEPP-2000", in *Proc. eeFACT'16*, Daresbury, UK (2016), p. 32.

[4] V.V. Danilov *et al*., "The Concept of Round Colliding Beams", in *Proc. EPAC'96*, Sitges, Spain, 1996, pp. 1149-1151.

[5] L.M. Barkov *et al.*, "Phi-Factory Project in Novosibirsk", in *Proc. 14th HEACC'89*, Tsukuba, Japan, 1989, p. 1385.

[6] K. Ohmi, K. Oide and E.A. Perevedentsev, "The beam-beam limit and the degree of freedom", in *Proc. EPAC'06*, Edinburgh, Scotland, 2006, pp.616-618.

[7] T.V. Dimova *et al.*, "Recent Results on e^+e^-→hadrons Cross Sections from SND and CMD-3 Detectors at VEPP-2000 collider", *Nucl. Part. Phys. Proc.*, vol. 273-275, pp. 1991-1996, 2016.

[8] A.A. Korol *et al.*, "Measurement of the hadronic cross sections with the CMD-3 and SND detectors at the VEPP-2000 collider", *EPJ Web of Conferences,* 182, 02068 (2017).

[9] D. Berkaev *et al.*, "VEPP-5 Injection Complex: Two Colliders Operation Experience", in *Proc. IPAC'17*, Copenhagen, Denmark, pp. 2982-2984.

[10] Yu. Maltseva *et al.*, "VEPP-5 Injection Complex: New Possibilities for BINP Electron-Positron Colliders", in *Proc. IPAC'18*, Vancouver, Canada, pp. 371-373.

[11] D. Shwartz *et al.*, "Booster of Electrons and Positrons (BEP) Upgrade to 1 GeV", in *Proc. IPAC'14*, Dresden, Germany, pp. 102-104.

[12] P.Yu. Shatunov *et al*., "Magnet Structure of the VEPP-2000 Electron-positron Collider", in *Proc. EPAC'06*, Edinburgh, Scotland, 2006, pp. 628-630.

[13] A.L. Romanov *et al*., "Round Beam Lattice Correction using Response Matrix at VEPP-2000", in *Proc. IPAC'10*, Kyoto, Japan, 2010, pp. 4542-4544.

[14] D. Shwartz *et al*., "Recent Beam-Beam Effects at VEPP-2000 and VEPP-4M", in *Proc. ICFA Mini-Workshop on Beam-Beam Effects in Hadron Colliders (BB2013)*, Geneva, Switzerland, 2013, CERN-2014-004, pp. 43-49.

[15] A.V. Otboyev and E.A. Perevedentsev. "On self-consistent β-functions of colliding bunches", in *Proc. PAC'1999*, New York, USA, 1999, pp. 1524-1526.

[16] Yu.A. Rogovsky *et al*., "Status and Perspectives of the VEPP-2000 Complex", in *Proc. RuPAC'14*, Obninsk, Russia, 2014, pp. 6-10.

[17] Yu.A. Rogovsky *et al*., "Current Dependence of Bunch Dimensions in VEPP-2000 Collider", in *Proc. RuPAC'18*, Protvino, Russia, 2018, THCEMH04.

[18] P.M. Ivanov *et al*., "Luminosity and the Beam-Beam Effects on the Electron-Positron Storage Ring VEPP-2M with Superconducting Wiggler Magnet", in *Proc. 3rd Advanced ICFA Beam Dynamics Workshop on Beam–Beam Effects in Circular Colliders*, Novosibirsk, USSR, 1989, pp. 26-33.

[19] G.M. Tumaikin, private communication.

[20] K. Hirata, "Coherent Betatron Oscillation Modes Due to Beam-Beam Interaction", *Nucl. Instrum. Methods Phys. Res. A* 269, 1988, pp. 1-22.

[21] K. Yokoya, H. Koiso, "Tune Shift of Coherent Beam-Beam Oscillations", *Particle Accelerators,* 1990, Vol.27, pp. 181-186.

[22] P.M. Ivanov *et al.*, "Experimental Studies of Beam–Beam Effects at VEPP-2M", *in Proc. Workshop on Beam–Beam Effects in Circular Colliders*, Fermilab, USA, 2001, p. 36.

[23] D. Shatilov, *Part. Accel.,* vol. 52, p. 65, 1996.

[24] D. Berkaev *et al.*, "Commissioning of Upgraded VEPP-2000 Injection Chain", in *Proc. IPAC'16*, Busan, Korea, pp. 3811-3813.

[25] D. Shwartz *et al.*, "Recomissioning and Perspectives of VEPP-2000 e+e– Collider", *PoS ICHEP2016* (2016), p.054.

[26] P. Shatunov *et al.*, "High Luminosity at VEPP-2000 Collider With New Injector", in *Proc. IPAC'17*, Copenhagen, Denmark, pp. 2989-2991.

[27] Yu. M. Shatunov *et al*., "Commissioning of the Electron-Positron Collider VEPP-2000 after the Upgrade", *Phys. Part. Nucl. Lett.* (2018) 15, pp. 310-314.

[28] R.R. Akhmetshin *et al.*, "Hadronic cross sections with the CMD-3 detector at the VEPP-2000", *Nucl. Part. Phys. Proc.,* 294-296 (2018) pp. 170-176.

[29] E.A. Kozyrev *et al.*, "Study of the process $e^+e^- \rightarrow K^+K^-$ in the center-of-mass energy range 1010–1060 MeV with the CMD-3 detector", *Phys. Lett. B,* 779 (2018) pp. 64-71.

[30] A.A. Korol *et al.*, "Recent Results from the SND Detector", *Phys. Part. Nucl.,* 49 (2018) pp. 730-734.

[31] M. Timoshenko *et al.*, "Development of longitudinal beam profile diagnostics for beam-beam effects study at VEPP-2000", in *Proc. IBIC'18*, Shanghai, China, paper WEPA18.